

Collins-Soper kernel from lattice QCD at close-to-physical pion mass

Artur Avkhadiev¹

in collaboration with

Phiala Shanahan¹, Michael Wagman², and Yong Zhao³

International Symposium on Lattice Field Theory
July 31–August 4, 2023

2023
LATTICE

arXiv:2307.12359

¹  Massachusetts
Institute of
Technology

²  Fermilab

³ Argonne 
NATIONAL LABORATORY

The Collins-Soper (CS) kernel

- Related to TMDs (transverse-momentum-dependent distributions): a generalization of hadronic structure functions, e.g. PDFs:

$$\text{PDFs } f_{q/h}(x, \mu) \longrightarrow \text{TMD PDFs } f_{q/h}(x, b_T, \mu, \zeta)$$

- Describes RG evolution of TMDs along ζ :

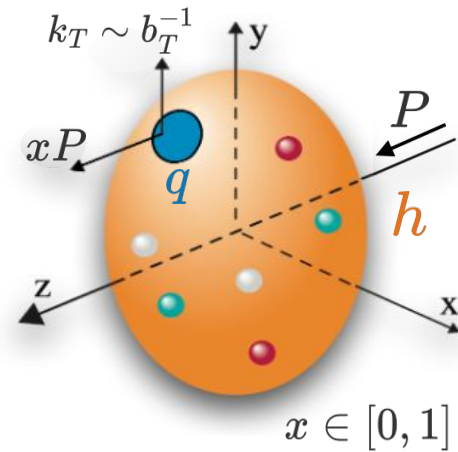
$$f_{q/h}(x, b_T, \mu, \zeta) = f_{q/h}(x, b_T, \mu, \zeta_0) \exp \left[\frac{1}{2} \gamma_q(b_T, \mu) \ln \frac{\zeta}{\zeta_0} \right]$$

- \Rightarrow Computed as a ratio of TMDs at different ζ :

- Independent of hadronic state (\Rightarrow choose pion)
- Non-perturbative at large b_T (for any μ)

$$\gamma_q(b_T, \mu) = \frac{2}{\ln(\zeta_1/\zeta_2)} \ln \frac{f_{q/h}(x, b_T, \mu, \zeta_1)}{f_{q/h}(x, b_T, \mu, \zeta_2)}$$

Proportional to hadron momentum P

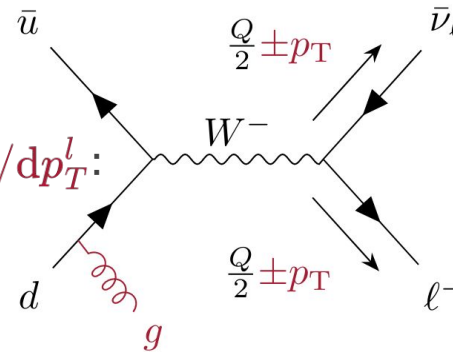


Based on Fig. 1.1 in TMD Handbook, 2304.03302

- Encoded by light-like matrix elements

Example: CS kernel in W mass measurement

- Extract M_W from $p\bar{p} \rightarrow W^- \rightarrow l^- \nu_l$ via lepton's $p_T^l + \text{template fits of } d\sigma/dp_T^l$:
- p_T^l depends on q_T : transverse momentum of the $\bar{u}d$ pair.



- Variations in CS kernel model \Rightarrow % variations in $d\sigma/dq_T$:

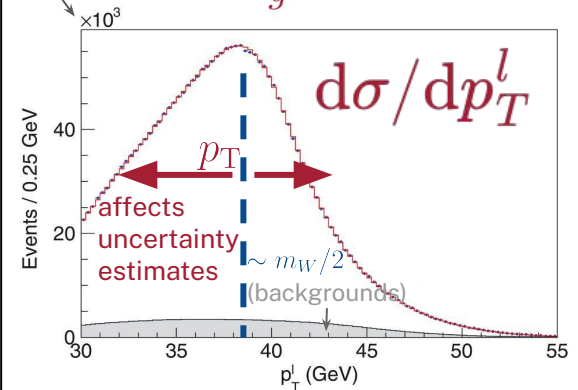
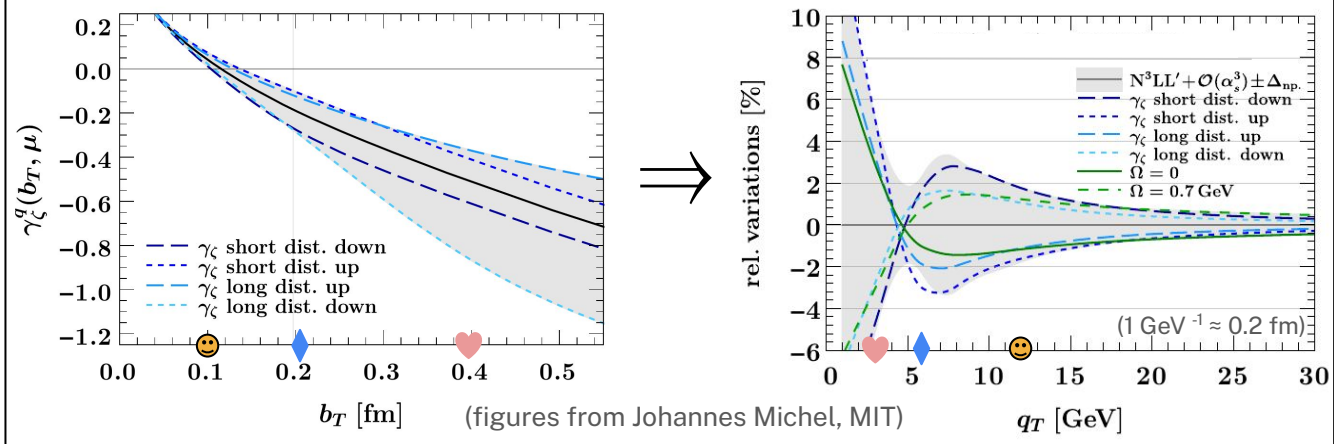
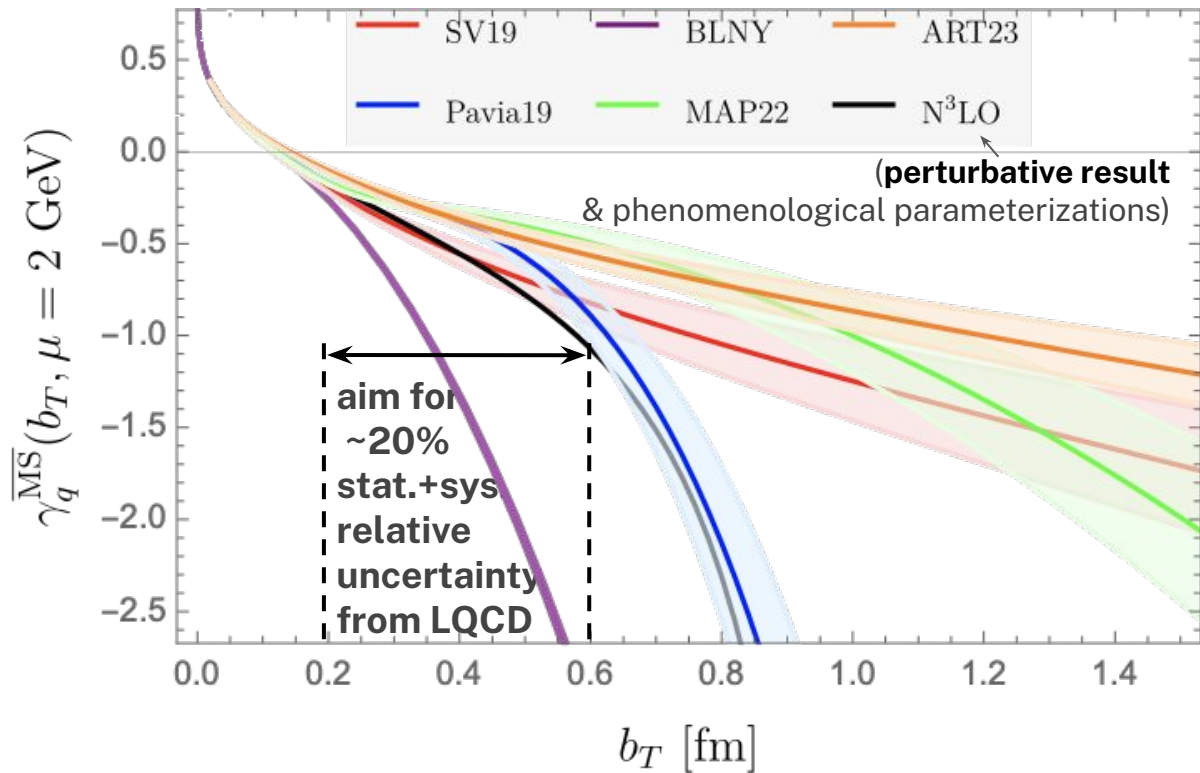


Fig. 4(B) from High-precision measurement of the W boson mass with the CDF II detector, CDF Collaboration et al., Science **376**, 170-176 (2022) (annotated for presentation)

- Non-perturbative CS kernel affects M_W measurement through the template shape for $d\sigma/dp_T^l$ (but not enough to explain the discrepancy).

Non-perturbative CS kernel

- Consistent for $b_T \lesssim 0.2 \text{ fm}$ ($\approx 1 \text{ GeV}^{-1}$)
- Non-perturbative modeling significant for $b_T \gtrsim 0.2 \text{ fm}$
- LQCD goal: sufficient precision for direct comparison



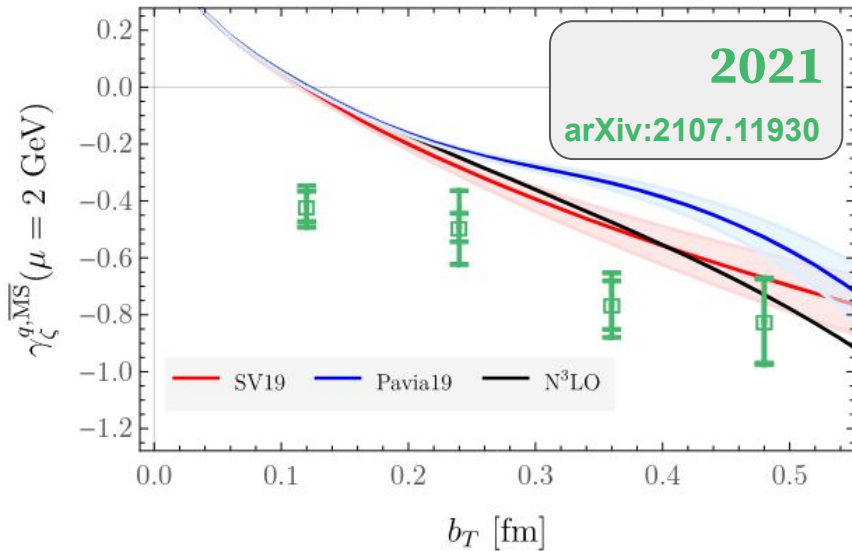
BLNY: F. Landry et. al, PRD 67 (2003), [hep-ph/0212159]
SV19: I. Scimemi and A. Vladimirov, JHEP 06, 137 [1912.06532]

Pavia19: A. Bacchetta et. al, JHEP 07, 117, [1912.07550]
MAP22: A. Bacchetta et. al, JHEP 10, 127, [2206.07598]
ART23: V. Moos et. al, [2305.07473]

Status of our group's calculations of the CS kernel

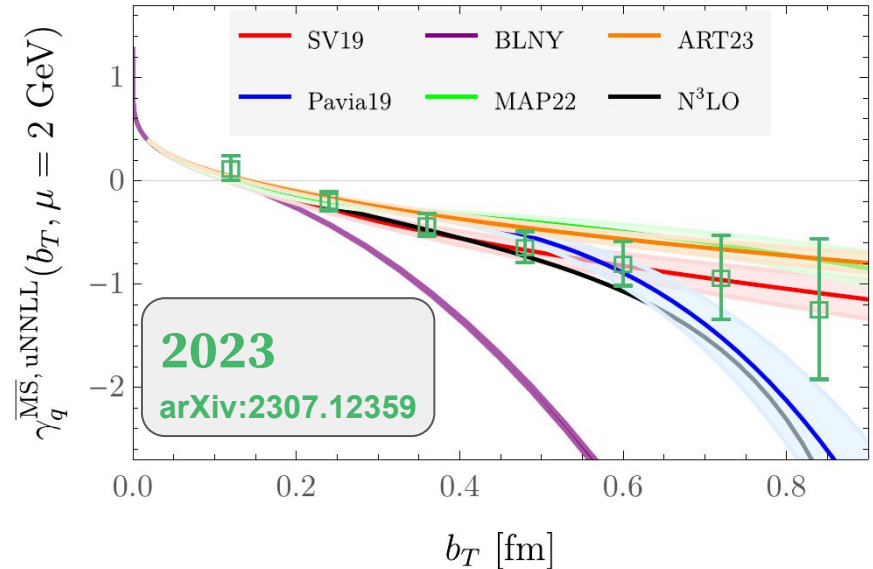
Proof of concept

- $M_\pi \approx 540$ MeV
- $0.12 \text{ fm} \leq b_T \leq 0.48 \text{ fm}$
- **NLO** matching.



Improved systematics

- $M_\pi \approx 150$ MeV
- $0.12 \text{ fm} \leq b_T \leq 0.86 \text{ fm}$ **Increased range**
- **NNLL** matching.



CS kernel from LQCD: outline

X. Ji et. al., Phys. Lett. B 811 [1911.03840]

$$\gamma_q(b_T, \mu) = \lim_{a \rightarrow 0} \frac{1}{\ln(P_1^z/P_2^z)} \ln \left[\frac{\int db^z e^{ib^z x P_1^z} P_1^z N_\Gamma(P_1^z) \sum_{\Gamma'} Z_{\Gamma\Gamma'}(\mu) \lim_{\ell \rightarrow \infty} W_{\Gamma'}^{(0)}(b^z, b_T, \ell, P_1^z)}{\int db^z e^{ib^z x P_2^z} P_2^z N_\Gamma(P_2^z) \sum_{\Gamma'} Z_{\Gamma\Gamma'}(\mu) \lim_{\ell \rightarrow \infty} W_{\Gamma'}^{(0)}(b^z, b_T, \ell, P_2^z)} \right]$$

2. Fourier transform

1. Quasi-TMDs in position space

+ $\delta\gamma_q(\mu, P_1^z, P_2^z)$ + p. c.

4. Power corrections

3. EFT matching

X. Ji et. al, PRD91 (2015);
 Ebert et. al, PRD99 (2019), JHEP09 (2019) 037;

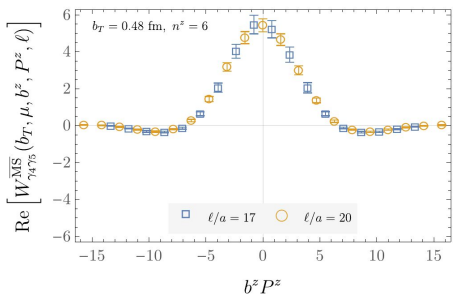
Calculations done on single 2+1+1 ensemble

- 48³ x 64, a = 0.12 fm
- Wilson-flowed
- Clover-on-HISQ

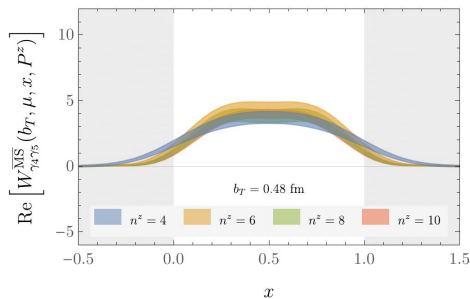
A. Bazavov et al. (MILC),
 PRD 87 (2013), [1212.4768]

CS kernel from LQCD: outline

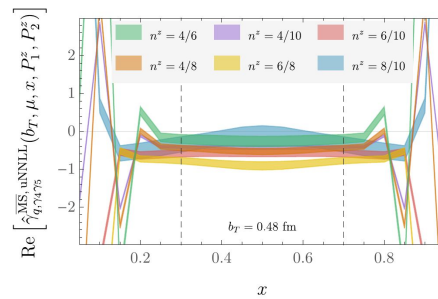
position-space MEs



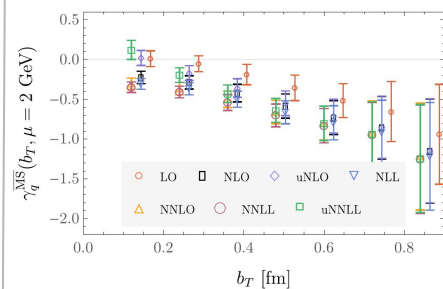
momentum-space MEs



ratios of MEs



...repeated for each bT



$$\sum_{\Gamma'} Z_{\Gamma\Gamma'}(\mu) \lim_{\ell \rightarrow \infty} W_{\mathcal{O}}^{\Gamma'}(b^z, b_T, \ell, P_1^z)$$

$$\int db^z e^{ib^z x P_1^z} P_1^z N_{\Gamma}(P_1^z)$$

$$\sum_{\Gamma'} Z_{\Gamma\Gamma'}(\mu) \lim_{\ell \rightarrow \infty} W_{\mathcal{O}}^{\Gamma'}(b^z, b_T, \ell, P_1^z)$$

$$\gamma_q(b_T, \mu) = \lim_{a \rightarrow 0} \frac{1}{\ln(P_1^z/P_2^z)} \ln \left[\frac{\int db^z e^{ib^z x P_1^z} P_1^z N_{\Gamma}(P_1^z)}{\int db^z e^{ib^z x P_2^z} P_2^z N_{\Gamma}(P_2^z)} \right] \sum_{\Gamma'} Z_{\Gamma\Gamma'}(\mu) \lim_{\ell \rightarrow \infty} W_{\mathcal{O}}^{\Gamma'}(b^z, b_T, \ell, P_1^z) + \delta\gamma_q(\mu, P_1^z, P_2^z) + \text{p. c.}$$

Position-space quasi-TMDs

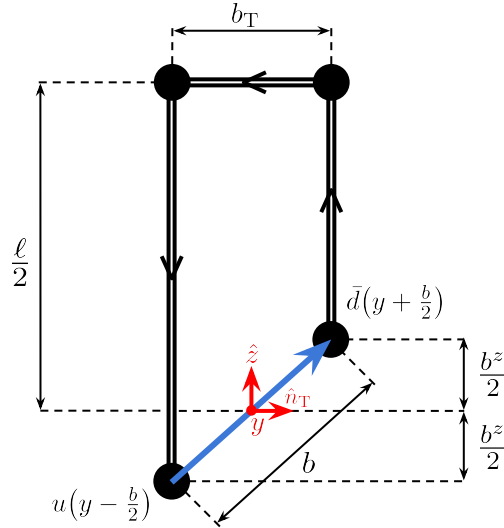
- Compute **quasi-TMD wavefunctions (WFs)**

$$\begin{aligned} \phi_{\Gamma}(b_T, b^z, P^z, \ell) \\ = \langle 0 | \mathcal{O}_{\Gamma}(b_T, b^z, 0, \ell) | \pi(P^z) \rangle \end{aligned}$$

- Operators

$$\mathcal{O}_{\Gamma}(b_T, b^z, y, \ell)$$

with staple-shaped Wilson lines:



- For each

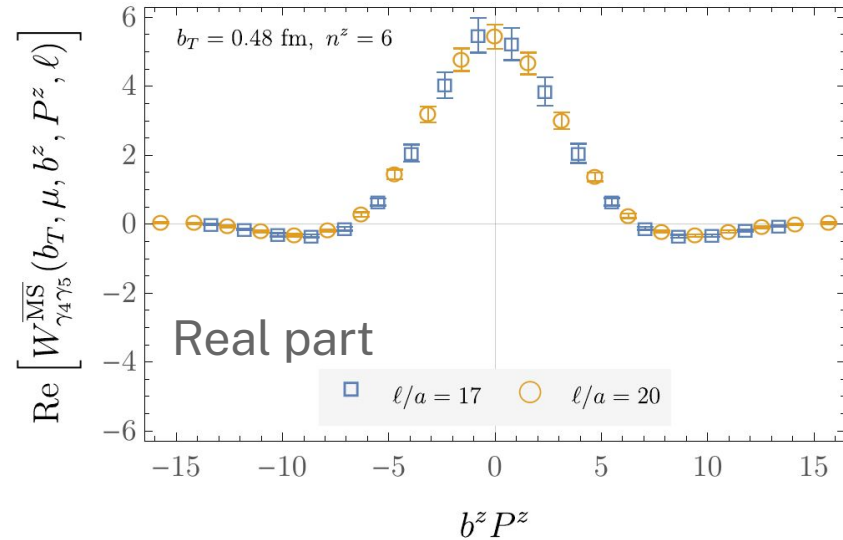
P^z, b_T, b^z, ℓ —
expensive!

- Matrix elements have divergences $\sim \ell + b_T$

$$\gamma_q(b_T, \mu) = \lim_{a \rightarrow 0} \frac{1}{\ln(P_1^z/P_2^z)} \ln \left[\frac{\int db^z e^{ib^z P_1^z} P_1^z N_{\Gamma}(P_1^z)}{\int db^z e^{ib^z P_2^z} P_2^z N_{\Gamma}(P_2^z)} \right] \frac{\sum_{\Gamma'} Z_{\Gamma'}(\mu) \lim_{\ell \rightarrow \infty} W_{\Gamma'}^{(0)}(b^z, b_T, \ell, P_1^z)}{\sum_{\Gamma'} Z_{\Gamma'}(\mu) \lim_{\ell \rightarrow \infty} W_{\Gamma'}^{(0)}(b^z, b_T, \ell, P_2^z)} + \delta\gamma_q(\mu, P_1^z, P_2^z) + \text{p. c.}$$

- Subtract divergences in **quasi-TMD WF ratios**

$$W_{\Gamma}^{(0)}(b_T, b^z, P^z, \ell) = \frac{\tilde{\phi}_{\Gamma}(b_T, b^z, P^z, \ell)}{\tilde{\phi}_{\gamma^4 \gamma^5}(b_T, 0, 0, \ell)}$$



Position-space quasi-TMDs

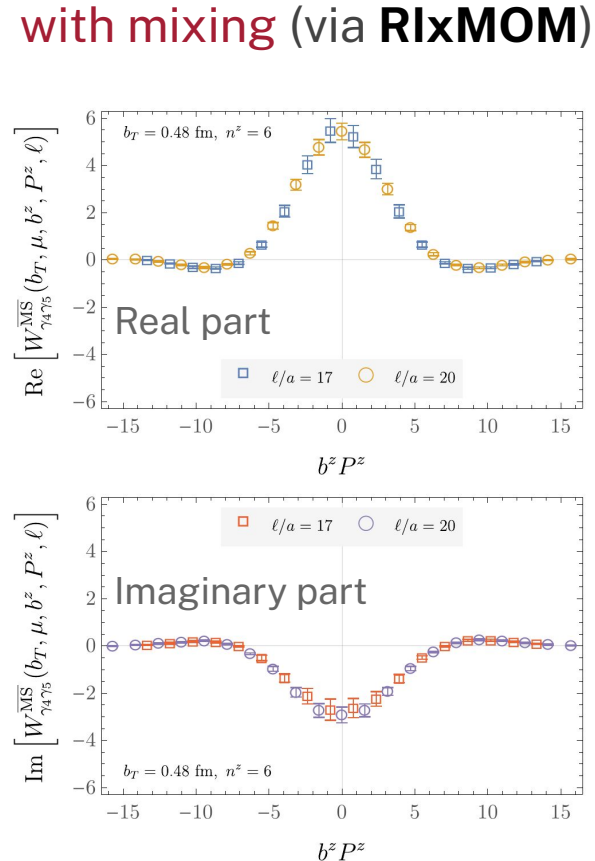
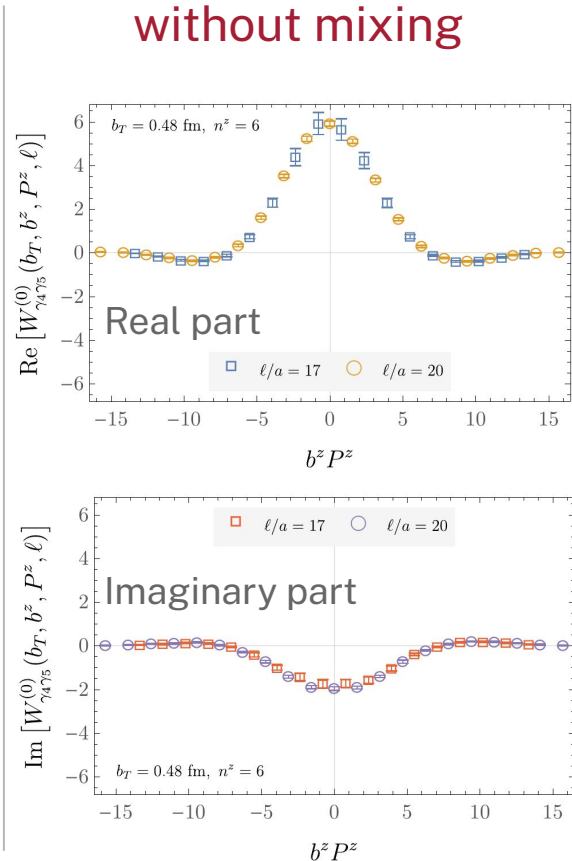
$$\gamma_q(b_T, \mu) = \lim_{a \rightarrow 0} \frac{1}{\ln(P_1^z/P_2^z)} \ln \left[\frac{\int db^z e^{ib^z x P_1^z} P_1^z N_\Gamma(P_1^z)}{\int db^z e^{ib^z x P_2^z} P_2^z N_\Gamma(P_2^z)} \sum_{\Gamma'} Z_{\Gamma\Gamma'}(\mu) \lim_{\ell \rightarrow \infty} W_{\Gamma'}^{(0)}(b^z, b_T, \ell, P_1^z) \right] + \delta\gamma_q(\mu, P_1^z, P_2^z) + \text{p.c.}$$

- Mixing effects included via **RlxMOM** scheme (in backup)

$$W_\Gamma^{\overline{\text{MS}}}(b_T, \mu, b^z, P^z, \ell) = \sum_{\Gamma'} Z_{\Gamma\Gamma'}^{\overline{\text{MS}}}(\mu) W_\Gamma^{(0)}(b_T, b^z, P^z, \ell)$$

$$\Gamma \in \{\gamma_4\gamma_5, \gamma_3\gamma_5\}$$

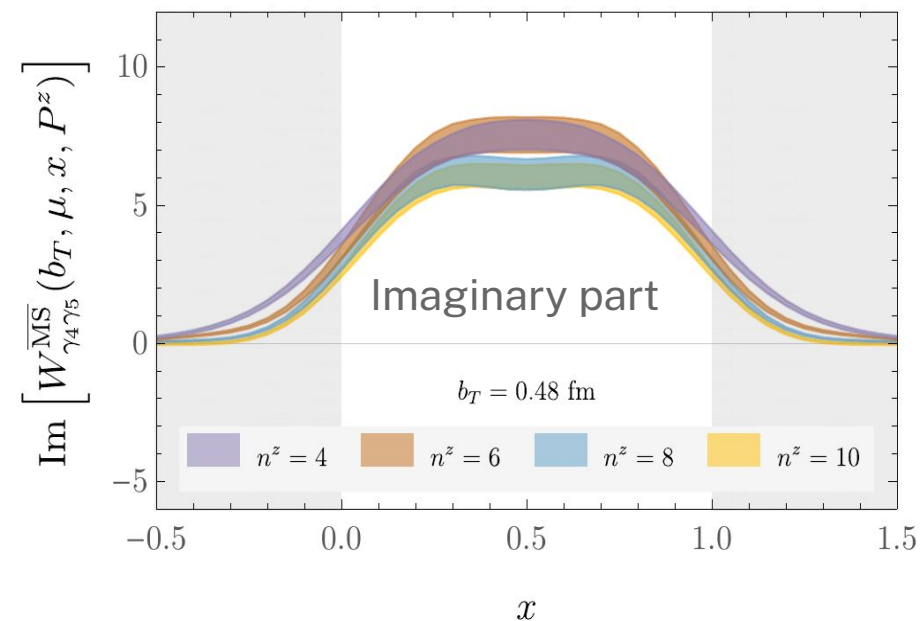
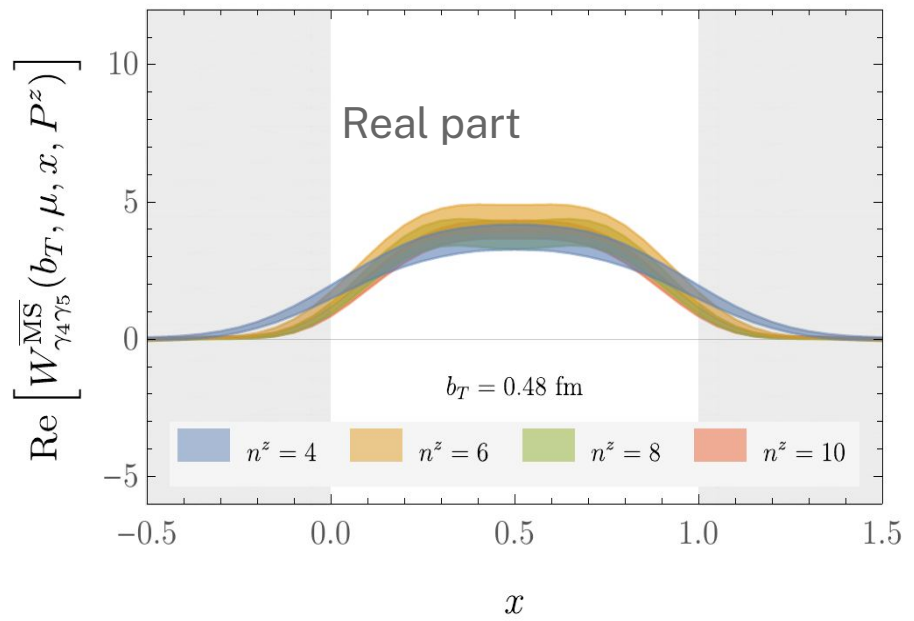
- Shown for $b_T = 0.48$ fm, $P_z = 1.29$ GeV.
- Consistent between different staple lengths ℓ .
- Decay to zero within computed b_z ranges.



Momentum-space quasi-TMDs

$$\gamma_q(b_T, \mu) = \lim_{a \rightarrow 0} \frac{1}{\ln(P_1^z/P_2^z)} \ln \left[\frac{\int db^z e^{ib^z x P_1^z} P_1^z N_\Gamma(P_1^z)}{\int db^z e^{ib^z x P_2^z} P_2^z N_\Gamma(P_2^z)} \right] \frac{\sum_{\Gamma'} Z_{\Gamma'}(\mu) \lim_{\ell \rightarrow \infty} W_{\Gamma'}^{(0)}(b^z, b_T, \ell, P_1^z)}{\sum_{\Gamma'} Z_{\Gamma'}(\mu) \lim_{\ell \rightarrow \infty} W_{\Gamma'}^{(0)}(b^z, b_T, \ell, P_2^z)} + \delta\gamma_q(\mu, P_1^z, P_2^z) + \text{p. c.}$$

- Have support outside $x \in [0, 1]$, as expected.
- Converge to physical range $x \in [0, 1]$ with increasing $P^z = \frac{2\pi}{L} n^z$.



CS kernel estimate

$$\hat{\gamma}_{\Gamma}^{\overline{\text{MS}}}(b_T, x, P_1^z, P_2^z, \mu)$$

$$= \frac{1}{\ln(P_1^z/P_2^z)} \ln \left[\frac{W_{\Gamma}^{\overline{\text{MS}}}(b_T, x, P_1^z, \ell)}{W_{\Gamma}^{\overline{\text{MS}}}(b_T, x, P_2^z, \ell)} \right]$$

$$+ \delta\gamma_q^{\overline{\text{MS}}}(x, P_1^z, P_2^z, \mu)$$

- Separate for each momentum pair, b_T , Dirac structure, and matching accuracy.
- Differ by power corrections:

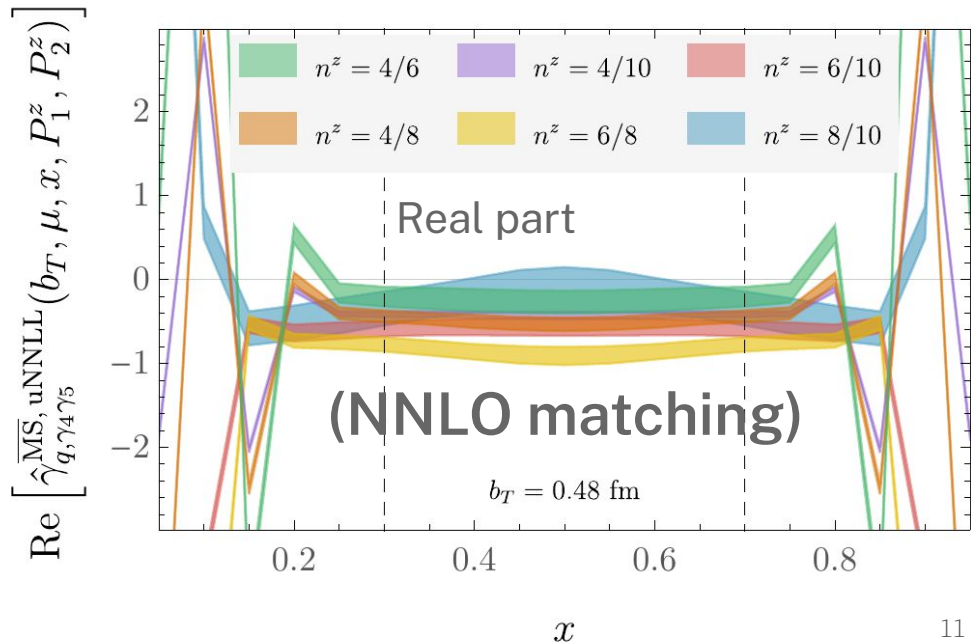
$$\mathcal{O} \left(\frac{1}{(xP^z b_T)^2}, \frac{m_{\pi}^2}{(xP^z)^2} \right) + (x \leftrightarrow 1-x)$$

P^z -dependent \Rightarrow cannot disentangle from $\mathcal{O}(a)$ effects at finite a .

X. Ji et al., Phys. Lett. B 811 [1911.03840]
 X. Ji and Y. Liu, PRD 105, [2106.05310]
 Z.-F. Deng et al, JHEP 09, [2207.07280]

$$\gamma_q(b_T, \mu) = \lim_{a \rightarrow 0} \frac{1}{\ln(P_1^z/P_2^z)} \ln \left[\frac{\int db^z e^{ib^z x P_1^z} P_1^z N_{\Gamma}(P_1^z)}{\int db^z e^{ib^z x P_2^z} P_2^z N_{\Gamma}(P_2^z)} \right] + \delta\gamma_q(\mu, P_1^z, P_2^z) + \text{p.c.}$$

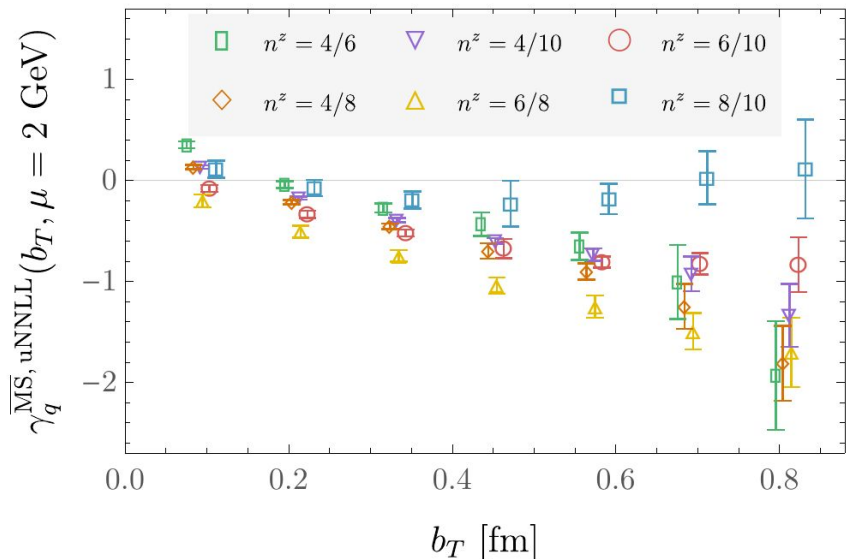
- Fit each estimator separately to a constant in $x \in [0.3, 0.7]$, then average fits at fixed b_T and matching accuracy.



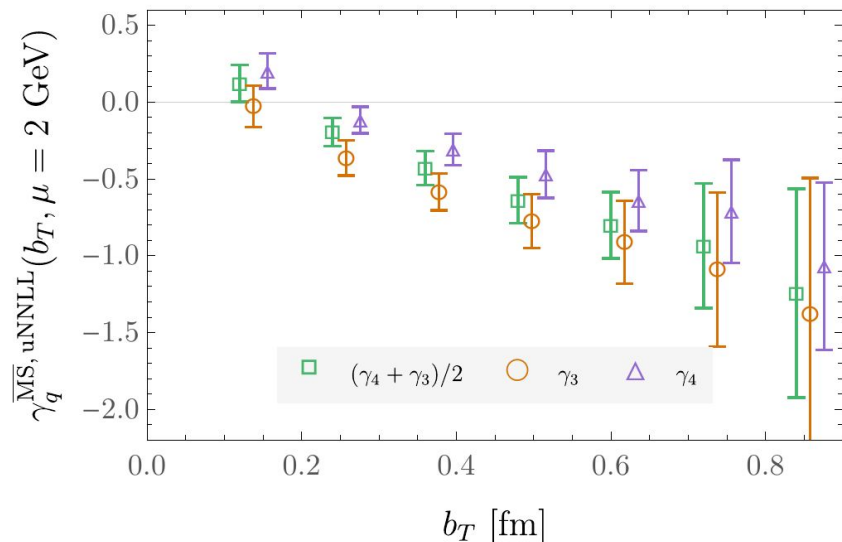
CS kernel estimate

$$\gamma_q(b_T, \mu) = \lim_{a \rightarrow 0} \frac{1}{\ln(P_1^z/P_2^z)} \ln \left[\frac{\int db^z e^{ib^z x P_1^z} P_1^z N_\Gamma(P_1^z)}{\int db^z e^{ib^z x P_2^z} P_2^z N_\Gamma(P_2^z)} \frac{\sum_{\Gamma'} Z_{\Gamma'}(\mu) \lim_{\ell \rightarrow \infty} W_{\Gamma'}^{(0)}(b^z, b_T, \ell, P_1^z)}{\sum_{\Gamma'} Z_{\Gamma'}(\mu) \lim_{\ell \rightarrow \infty} W_{\Gamma'}^{(0)}(b^z, b_T, \ell, P_2^z)} \right] + \delta\gamma_q(\mu, P_1^z, P_2^z) + \text{p. c.}$$

Before averaging over momentum pairs:



Before averaging over Dirac structures:



Matching corrections

- New results at **NNLO** and **NNLL**.
O. del Río and A. Vladimirov, [2304.14440], and X. Ji et. al, [2305.04416].

- $b_T \gtrsim 0.36$ fm: consistent between matching corrections above LO.

- $b_T \lesssim 0.36$ fm: deviations related to power corrections:

$$\mathcal{O}\left(\frac{1}{(P^z b_T)^2}\right)$$

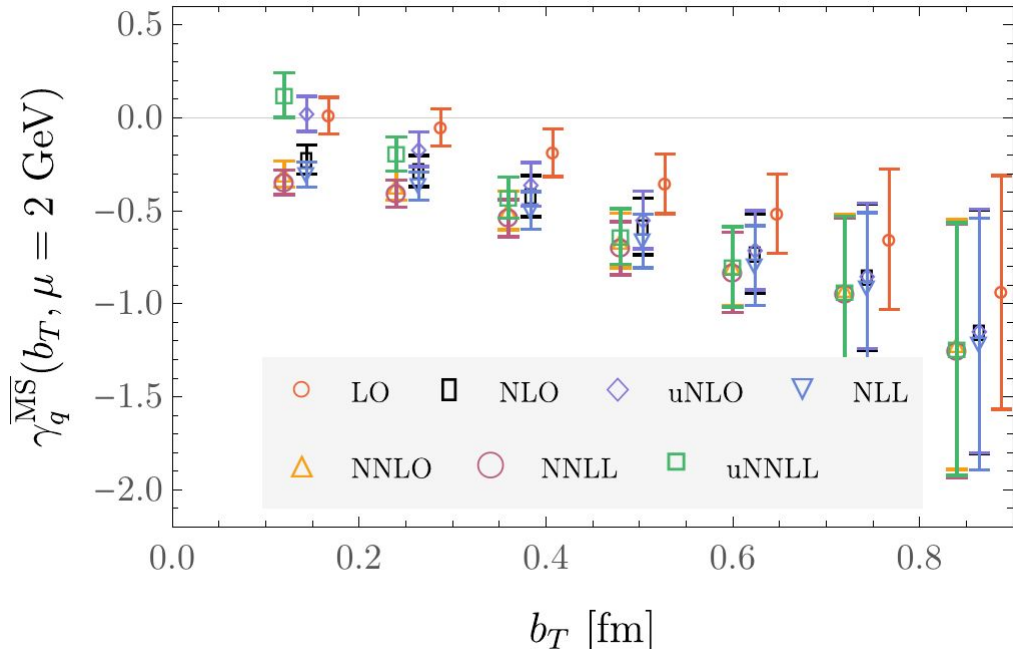
- Power corrections reduced by **uNLO**:

$$\delta\gamma_q^{\text{NLO}}(\mu, P_1^z, P_2^z) + \text{p.c.}$$

$$= \delta\gamma_q^{\text{uNLO}}(b_T, \mu, P_1^z, P_2^z) + \text{p.c.}'$$

incorporates some of the b_T -dependent power corrections in **p.c.** (more in backup)

$$\gamma_q(b_T, \mu) = \lim_{a \rightarrow 0} \frac{1}{\ln(P_1^z/P_2^z)} \ln \left[\frac{\int db^z e^{ib^z x P_1^z} P_1^z N_\Gamma(P_1^z)}{\int db^z e^{ib^z x P_2^z} P_2^z N_\Gamma(P_2^z)} \frac{\sum_{\Gamma'} Z_{\Gamma'}(\mu) \lim_{\ell \rightarrow \infty} W_{\Gamma'}^{(0)}(b^z, b_T, \ell, P_1^z)}{\sum_{\Gamma'} Z_{\Gamma'}(\mu) \lim_{\ell \rightarrow \infty} W_{\Gamma'}^{(0)}(b^z, b_T, \ell, P_2^z)} \right] + \delta\gamma_q(\mu, P_1^z, P_2^z) + \text{p.c.}$$



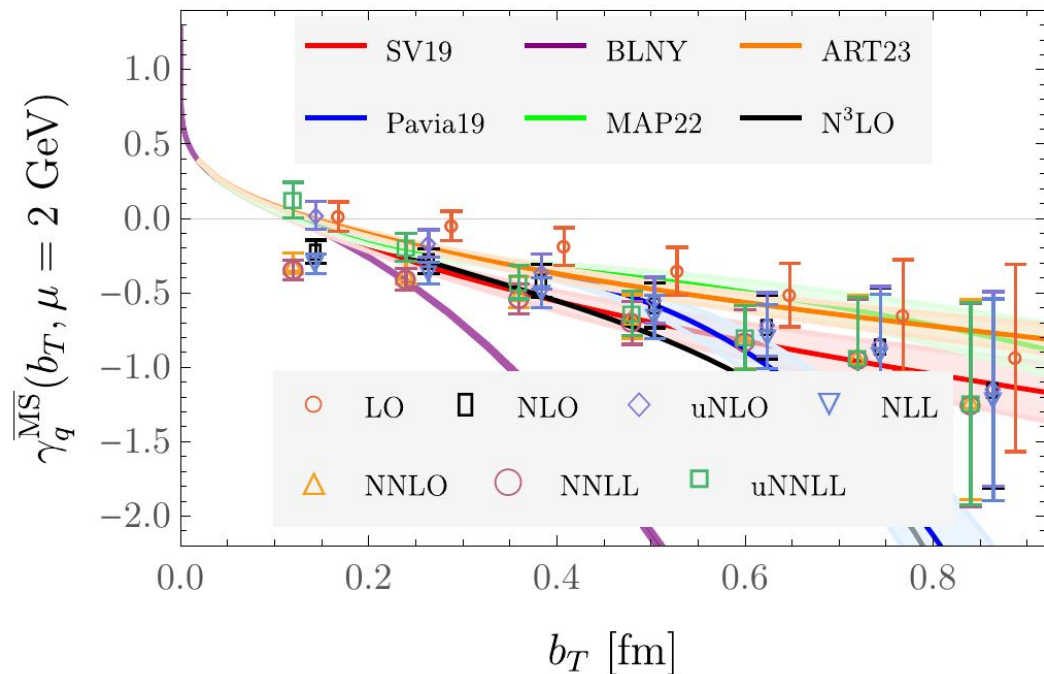
Final determination:

uNNLL = uNLO + resummation

Conclusion and outlook

- First calculation at \sim physical pion mass and **NNLO** + **NNLL** matching.
- Can begin to discriminate between phenomenological parameterizations.
- Perturbative convergence for $b_T > .36$ fm.
- Power corrections for $b_T < .36$ fm accounted by **uNLO**, **uNNLL**.
- **Significant progress from the 2021 calculation.**
- Next steps: better quantify power corrections by disentangling $O(a)$ effects at multiple lattice spacings.

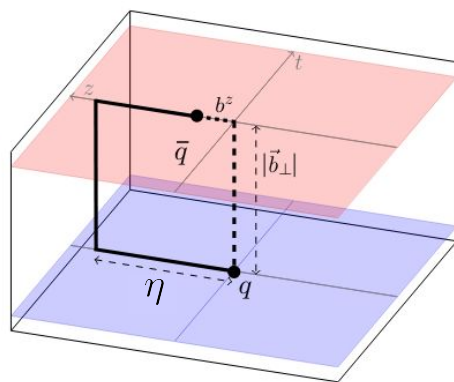
$$\gamma_q(b_T, \mu) = \lim_{a \rightarrow 0} \frac{1}{\ln(P_1^z/P_2^z)} \ln \left[\frac{\int db^z e^{ib^z x P_1^z} P_1^z N_\Gamma(P_1^z)}{\int db^z e^{ib^z x P_2^z} P_2^z N_\Gamma(P_2^z)} \sum_{\Gamma'} Z_{\Gamma'}(\mu) \lim_{\ell \rightarrow \infty} W_{\Gamma'}^{(0)}(b^z, b_T, \ell, P_1^z) \right] + \delta\gamma_q(\mu, P_1^z, P_2^z) + \text{p. c.}$$



Backup slides

CS Kernel from Lattice QCD

- CS kernel defined through ratios of **light-like MEs** of staple-shaped operators.
- Corresponding **space-like MEs** computed in LQCD, then matched onto the **light-like MEs** via Large-Momentum Effective Theory (LaMET).



Lorentz boost
and $\eta \rightarrow \infty$

$$\frac{1}{P} \ll b_T \ll \eta$$

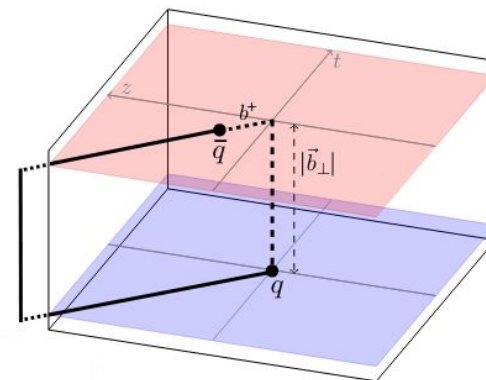


Fig. by Ebert, Stewart, Zhao, JHEP 1909 (2019)
(notation changed).

Ji, Sun, Xiong and Yuan, PRD91 (2015);
Ji, Jin, Yuan, Zhang and Zhao, PRD99 (2019);
Ebert, Stewart, Zhao, PRD99 (2019), JHEP09 (2019) 037;
Ji, Liu and Liu, NPB 955 (2020), PLB 811 (2020);
Vladimirov and Schäfer, PRD 101 (2020);
Ebert, Schindler, Stewart and Zhao, JHEP04 (2022) 178.

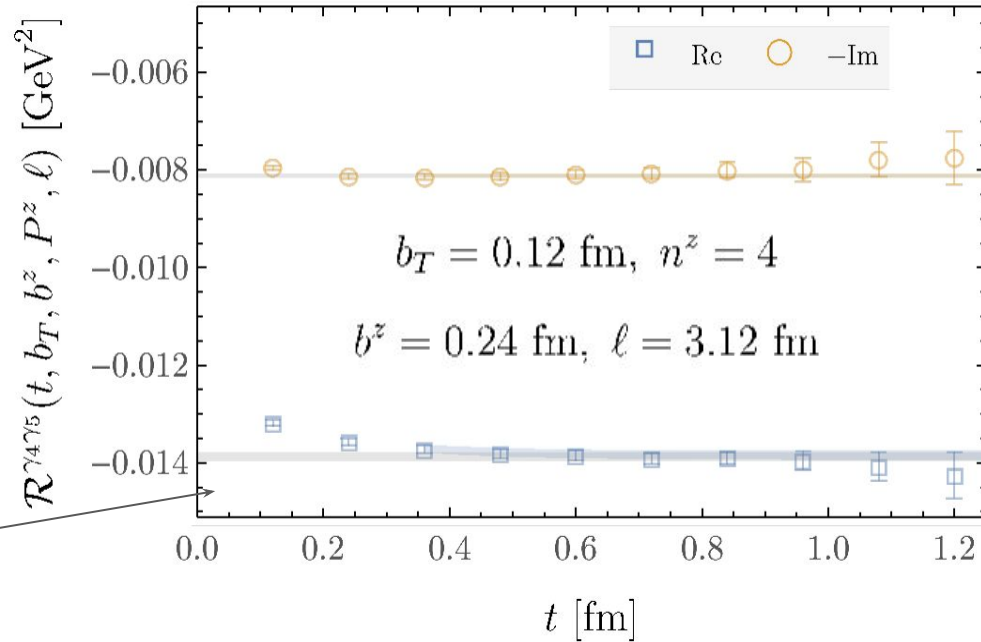
Unsubtracted quasi-TMD WFs: examples

- Extracted from correlation functions

$$\sum_{\mathbf{y}} e^{i\mathbf{P}\cdot\mathbf{y}} \left\langle \mathcal{O}_{\Gamma}(b_T, b^z, \mathbf{y}, \ell) \chi_{\mathbf{P}}^{\dagger}(0) \right\rangle$$

$$\xrightarrow{t \gg 0} \frac{Z_{\pi}^S(\mathbf{P})}{2E_{\pi}(\mathbf{P})} \tilde{\phi}_{\Gamma}(b_T, b^z, \mathbf{P}, \ell) e^{-E_{\pi}(\mathbf{P})t}$$

- Momentum-smeared interpolators $\chi_{\mathbf{P}}^{\dagger}$
- $E_{\pi}(\mathbf{P})$ and $Z_{\pi}^S(\mathbf{P})$ fit and cancelled in ratios $\mathcal{R}^{\Gamma}(t, b_T, b^z, P^z, \ell)$:
- Plateau gives $\tilde{\phi}_{\Gamma}(b_T, b^z, \mathbf{P}, \ell)$.
- Repeated for each P^z, b_T, b^z, ℓ .



- A range of time windows chosen systematically
- Covariance matrix from bootstrap + linear shrinkage
- Correlated determinations between staple geometries
- AIC-preferred fits (1 + 2 state)
- Further selection cuts + combine in weighted average

Mixing effects quantified with RIxMOM

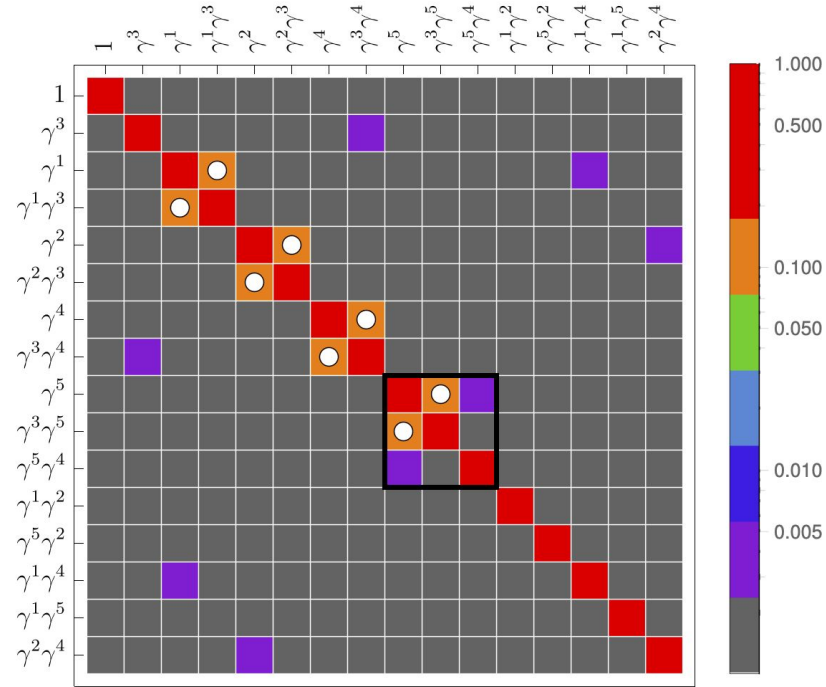
- Calculation of mixing effects in RIxMOM independent of staple geometry.

$$W_{\Gamma}^{\overline{\text{MS}}}(b_T, \mu, b^z, P^z, \ell) = \sum_{\Gamma'} Z_{\Gamma\Gamma'}^{\overline{\text{MS}}}(\mu) W_{\Gamma}^{(0)}(b_T, b^z, P^z, \ell)$$

- Full 16x16 mixing matrix computed

$$\mathcal{M}_{\Gamma\Gamma'}^{\text{RI/xMOM}}(p_R, \xi_R, a) \equiv \frac{\text{Abs}[Z_{\Gamma\Gamma'}^{\text{RI/xMOM}}(p_R, \xi_R, a)]}{\frac{1}{16} \sum_{\Gamma} \text{Abs}[Z_{\Gamma\Gamma}^{\text{RI/xMOM}}(p_R, \xi_R, a)]}$$

- Dominant mixings consistent with lattice perturbation theory at 1-loop.*



$$p_R^\mu = \frac{2\pi}{L} \times (0, 0, 10, 0), \quad \xi = 0.24 \text{ fm}$$

X. Ji, et. al, PRL 120 (2018), [1706.08962]

*M. Constantinou et al., PRD 99 (2019), [1901.03862]

J. Green et. al, PRL 121 (2018), [1707.07152]

Y. Ji et. al., PRD 104 (2021), [2104.13345]

J. Green et. al, PRD 101 (2020), [2002.09408]

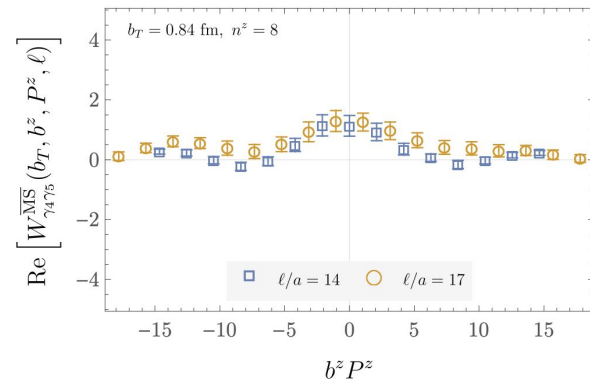
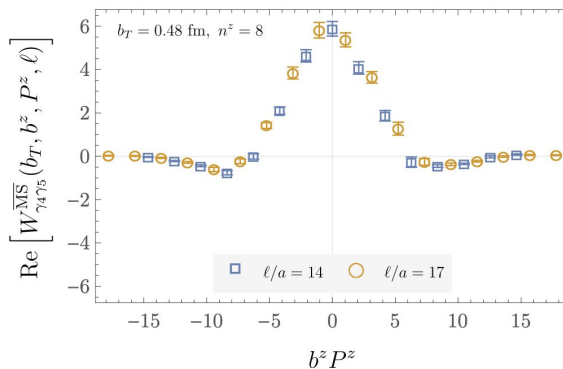
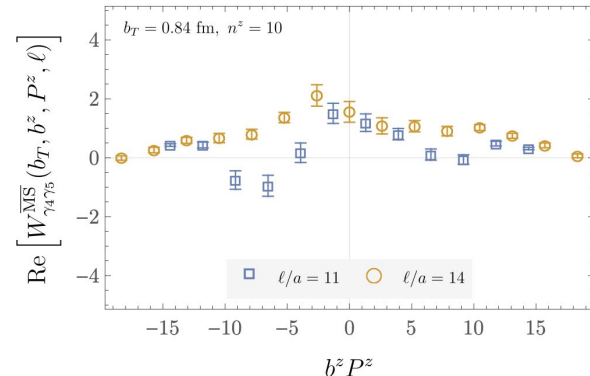
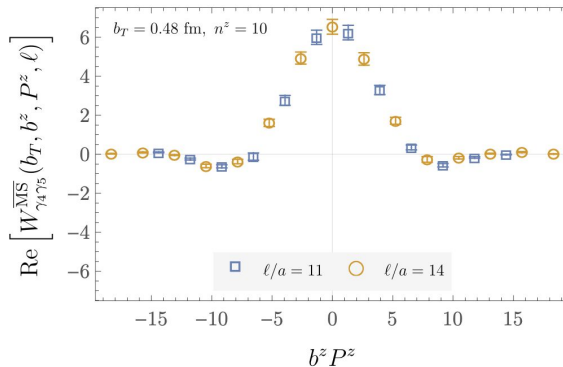
C. Alexandrou et al., [2305.11824]

TMD WFs in position space

$$\gamma_q(\mu, b_T) = \lim_{a \rightarrow 0} \frac{1}{\ln(P_1^z/P_2^z)} \ln \left[\frac{\int db^z e^{ib^z x P_1^z} \sum_{\Gamma'} Z_{\Gamma'}(\mu, a) \lim_{\ell \rightarrow \infty} W_O^{\Gamma'}(b^z, b_T, \ell, P_1^z, a)}{\int db^z e^{ib^z x P_2^z} \sum_{\Gamma'} Z_{\Gamma'}(\mu, a) \lim_{\ell \rightarrow \infty} W_O^{\Gamma'}(b^z, b_T, \ell, P_2^z, a)} \right] + \delta\gamma_q(\mu, b_T, P_1^z, P_2^z) + \mathcal{O}\left(\frac{1}{(xP^z b_T)^2}, \frac{M^2}{(xP^z)^2}, \frac{\Lambda_{\text{QCD}}^2}{(xP^z)^2}\right)$$

Statistical noise makes computation challenging for large P^z , ℓ , and b_T

- $b_T = 0.48 \text{ fm}, 0.84 \text{ fm}$
left to right
- $P^z = 2.15 \text{ GeV}, 1.72 \text{ GeV}$
top to bottom
- Our group's previous calculation had
 $b_T^{\text{max}} = 0.48 \text{ fm},$
 $P_{\text{max}}^z = 1.51 \text{ GeV}$



TMD WFs in momentum space

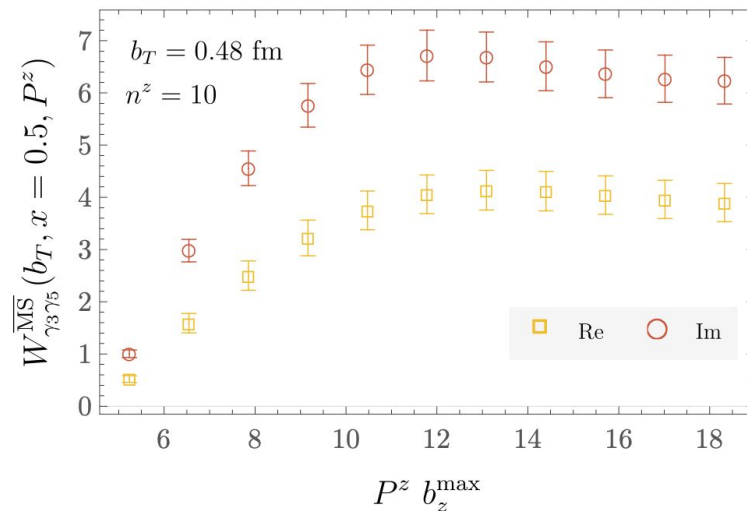
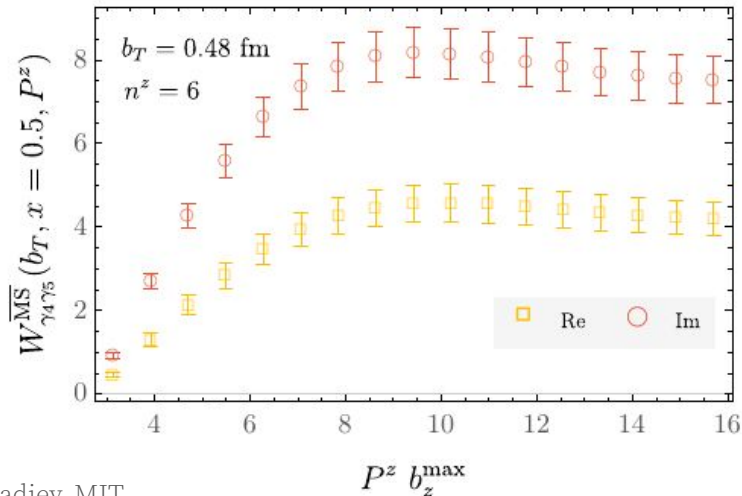
$$\gamma_q(\mu, b_T) = \lim_{a \rightarrow 0} \frac{1}{\ln(P_1^z/P_2^z)} \ln \left[\frac{\int db^z e^{ib^z x P_1^z} P_1^z \sum_{\Gamma'} Z_{\Gamma'}(\mu, a) \lim_{\ell \rightarrow \infty} W_O^{\Gamma'}(b^z, b_T, \ell, P_1^z, a)}{\int db^z e^{ib^z x P_2^z} P_2^z \sum_{\Gamma'} Z_{\Gamma'}(\mu, a) \lim_{\ell \rightarrow \infty} W_O^{\Gamma'}(b^z, b_T, \ell, P_2^z, a)} \right] + \delta\gamma_q(\mu, b_T, P_1^z, P_2^z) + \mathcal{O}\left(\frac{1}{(xP^z b_T)^2}, \frac{M^2}{(xP^z)^2}, \frac{\Lambda_{\text{QCD}}^2}{(xP^z)^2}\right)$$

bz range sufficient to use a Discrete Fourier Transform

$$\bar{W}_{\Gamma}^{\overline{\text{MS}}}(b_T, \mu, x, P^z) = \frac{P^z}{2\pi} N_{\Gamma}(P) \sum_{|b_z| \leq b_z^{\max}} e^{i(x-\frac{1}{2})P^z b^z} \bar{W}_{\Gamma}^{\overline{\text{MS}}}(b_T, \mu, b^z, P^z)$$

Normalization factor to compare between Dirac structures

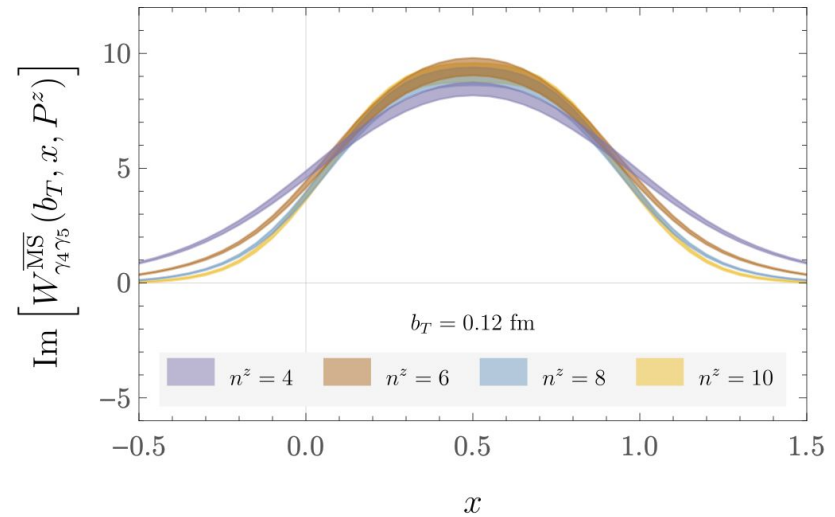
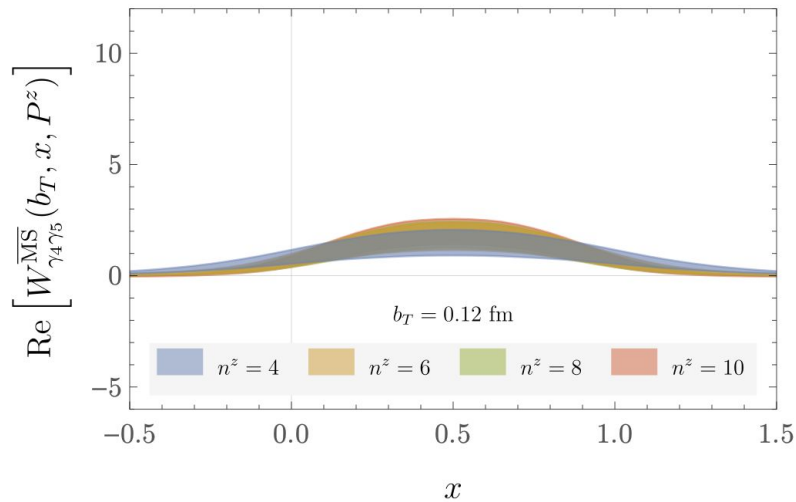
The DFT is stable to decreasing the range in b_T^{\max} :



TMD WFs in momentum space

$$\gamma_q(\mu, b_T) = \lim_{a \rightarrow 0} \frac{1}{\ln(P_1^z/P_2^z)} \ln \frac{\int db^z e^{ib^z x P_1^z} P_1^z \sum_{\Gamma'} Z_{\Gamma'}(\mu, a) \lim_{\ell \rightarrow \infty} W_O^{\Gamma'}(b^z, b_T, \ell, P_1^z, a)}{\int db^z e^{ib^z x P_2^z} P_2^z \sum_{\Gamma'} Z_{\Gamma'}(\mu, a) \lim_{\ell \rightarrow \infty} W_O^{\Gamma'}(b^z, b_T, \ell, P_2^z, a)} + \delta\gamma_q(\mu, b_T, P_1^z, P_2^z) + \mathcal{O}\left(\frac{1}{(xP^z b_T)^2}, \frac{M^2}{(xP^z)^2}, \frac{\Lambda_{\text{QCD}}^2}{(xP^z)^2}\right)$$

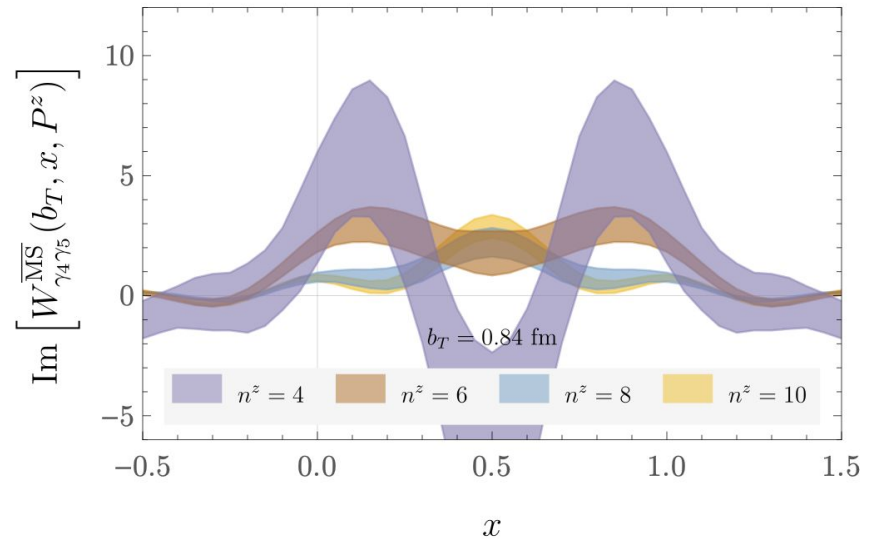
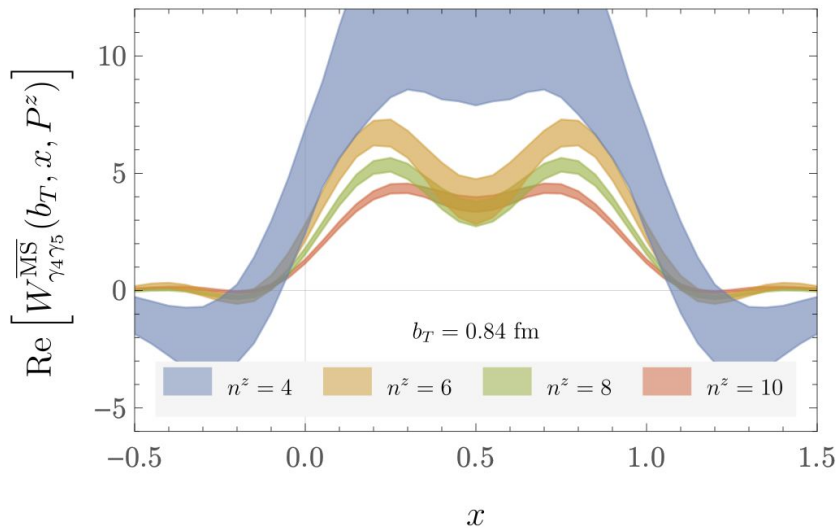
See convergence to the physical range $x \in [0, 1]$ with increasing $P^z = \frac{2\pi}{L} n^z$



TMD WFs in momentum space

$$\gamma_q(\mu, b_T) = \lim_{a \rightarrow 0} \frac{1}{\ln(P_1^z/P_2^z)} \ln \frac{\int db^z e^{ib^z x P_1^z} P_1^z \sum_{\Gamma'} Z_{\Gamma'}(\mu, a) \lim_{\ell \rightarrow \infty} W_O^{\Gamma'}(b^z, b_T, \ell, P_1^z, a)}{\int db^z e^{ib^z x P_2^z} P_2^z \sum_{\Gamma'} Z_{\Gamma'}(\mu, a) \lim_{\ell \rightarrow \infty} W_O^{\Gamma'}(b^z, b_T, \ell, P_2^z, a)} + \delta\gamma_q(\mu, b_T, P_1^z, P_2^z) + \mathcal{O}\left(\frac{1}{(xP^z b_T)^2}, \frac{M^2}{(xP^z)^2}, \frac{\Lambda_{\text{QCD}}^2}{(xP^z)^2}\right)$$

See convergence to the physical range $x \in [0, 1]$ with increasing $P^z = \frac{2\pi}{L} n^z$



NLO, NNLO, and resummations

The correction is given by coefficients

$$\delta\gamma_q(x, P_1^z, P_2^z, \mu) \equiv \frac{1}{\ln(P_1^z/P_2^z)} \left(\ln \frac{C_\phi(xP_2^z, \mu)}{C_\phi(xP_1^z, \mu)} + (x \leftrightarrow \bar{x}) \right)$$

$C_\phi(p^z, \mu)$ appear in the TMD WF matching formula and are computed perturbatively as

$$C_\phi(p^z, \mu) = 1 + \sum_{n=1} \left(\frac{\alpha_s(\mu)}{4\pi} \right)^n C_\phi^{(n)}(p^z, \mu)$$

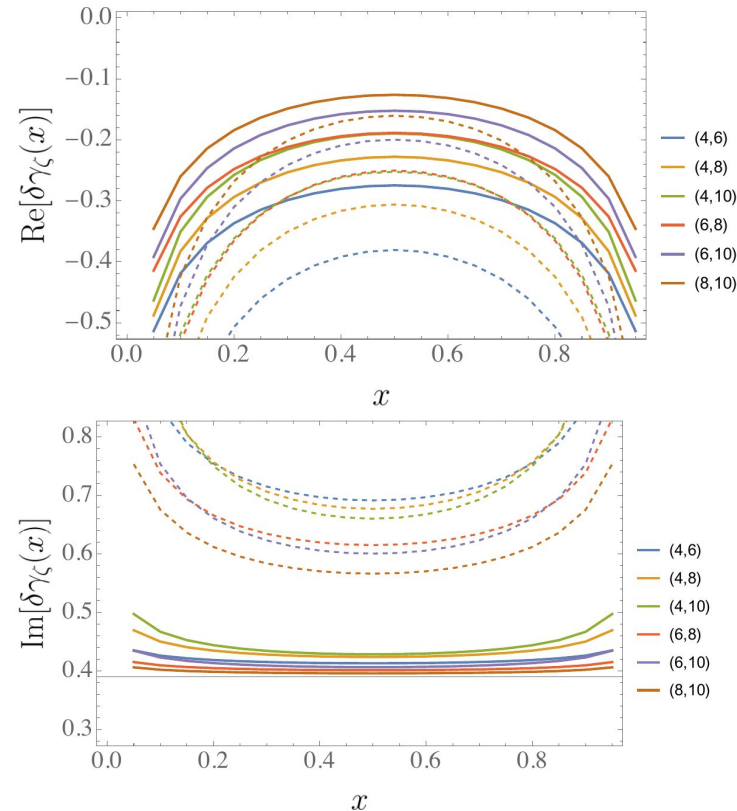
at LO, NLO and recently at NNLO, and resummed as

O. del Río and A. Vladimirov, [2304.14440]

X. Ji et. al, [2305.04416]

$$C_\phi(p^z, \mu) = C_\phi(p^z, 2p^z) \times \exp[K_\phi(p^z, 2p^z)]$$

Resummation kernel



NLO (solid) and NNLO (dashed);
No convergence in the imaginary part 23

NLL and NNLL

X. Ji et. al., Phys. Lett. B 811 [1911.03840]
 Ebert et. al, JHEP 04 (2022), [2201.08401]

Resummation kernel is $K_\phi(2p^z, \mu) = 2K_\Gamma(2p^z, \mu) - K_{\gamma_\mu}(2p^z, \mu) - i\pi\eta(2p^z, \mu)$

$$K_{\gamma_\mu}(\mu_0, \mu) = \int_{\alpha_s(\mu_0)}^{\alpha_s(\mu)} \frac{d\alpha_s}{\beta(\alpha_s)} \gamma_\mu(\alpha_s),$$

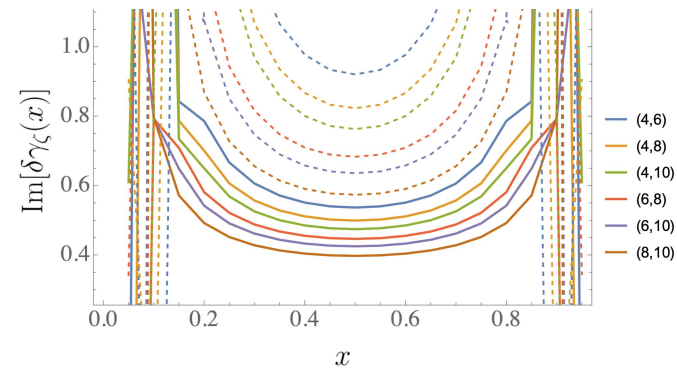
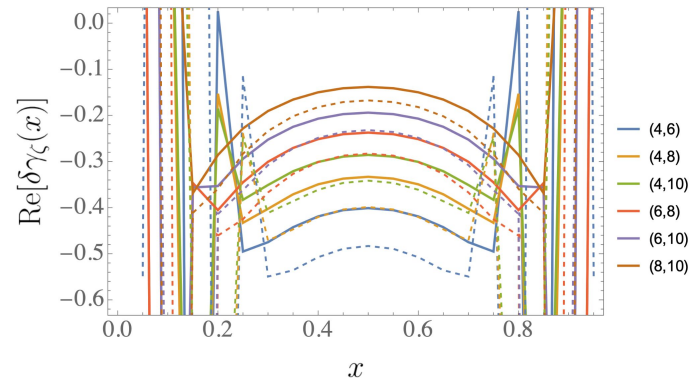
$$K_\Gamma(\mu_0, \mu) = \int_{\alpha_s(\mu_0)}^{\alpha_s(\mu)} \frac{d\alpha_s}{\beta(\alpha_s)} \Gamma_{\text{cusp}}(\alpha_s) \int_{\alpha_s(\mu_0)}^{\alpha_s} \frac{d\alpha'_s}{\beta(\alpha'_s)},$$

$$\eta_\Gamma(\mu_0, \mu) = \int_{\alpha_s(\mu_0)}^{\alpha_s(\mu)} \frac{d\alpha_s}{\beta(\alpha_s)} \Gamma_{\text{cusp}}(\alpha_s)$$

where $\Gamma_{\text{cusp}}(\alpha_s(\mu)) = \frac{d\gamma_\mu(p^z, \mu)}{d \ln p^z}$ and $\gamma_\mu(p^z, \mu) \equiv \frac{d \ln C_\phi(p^z, \mu)}{d \ln \mu}$

are computed perturbatively at following loop orders for each resummation accuracy:

| | K_Γ | K_{γ_C} | K_{γ_μ} | η | C_ϕ |
|------|------------|----------------|------------------|--------|----------|
| NLL | 2 | 1 | 1 | 1 | 0 |
| NNLL | 3 | 2 | 2 | 2 | 1 |



NLL (solid) and NNLL (dashed)
No convergence in the imaginary part

bT-dependent matching

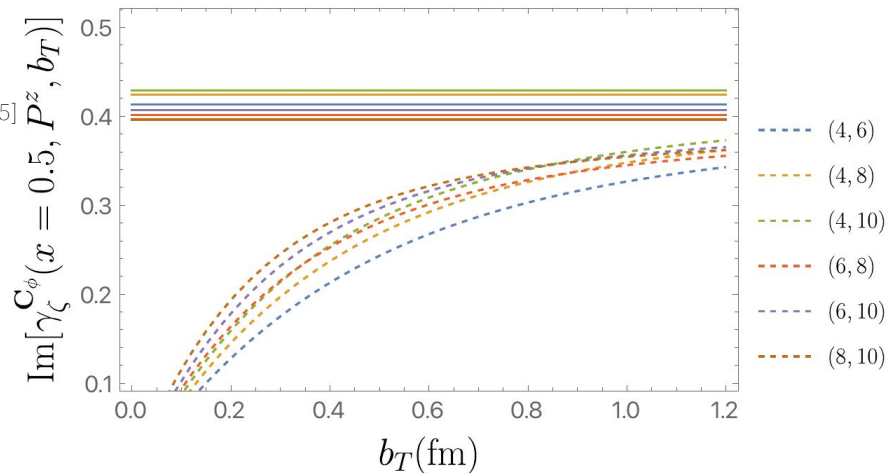
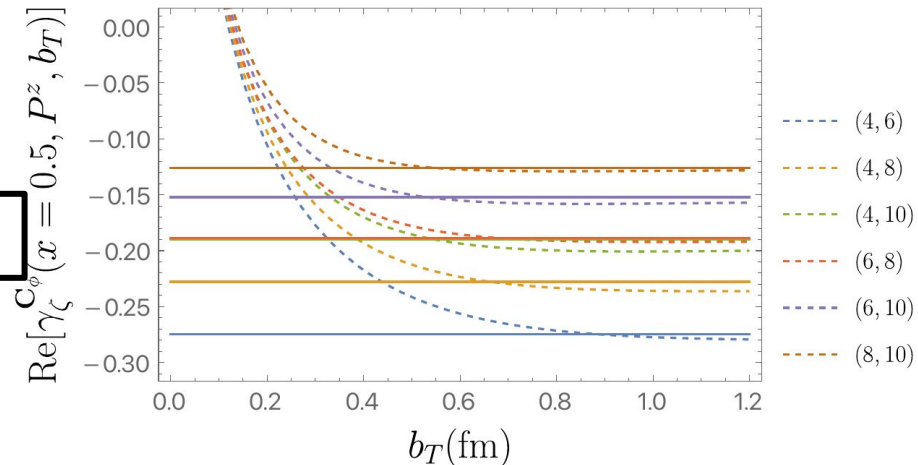
Matching coefficients C include are a $P^z b_T \gg 1$ limit of

$$\mathbf{C}_\phi(p^z, b_T, \mu) = C_\phi(p^z, \mu) + \delta C_\phi(p^z, b_T)$$

uNLO

$$p^z \in xP^z, \bar{x}P^z$$

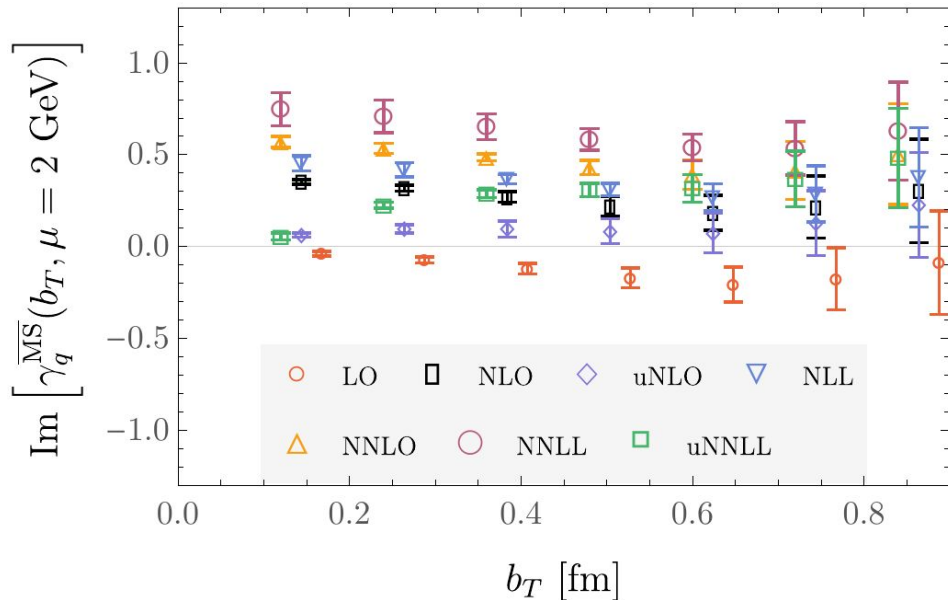
- $\delta C_\phi(p^z, b_T)$ contains bT-dependent terms on $x \in (-\infty, \infty)$ suppressed in $P^z b_T$
- Has been computed at NLO.
 - M. A. Ebert et. al., JHEP 09, 037, [1901.03685]
 - Z.-F. Deng et. al, JHEP 09, [2207.07280]
- Corresponding unexpanded (in bT) matching correction reveals power corrections in $1/P^z b_T$.
- Imaginary part more sensitive to power corrections => not taken as a systematic uncertainty directly.
 - M.-H. Chu et al. (LPC), PRD 106, 034509, [2204.00200]
 - M.-H. Chu et al. (LPC), [2302.09961]
 - M.-H. Chu et al. (LPC), [2306.06488]



Dashed: **uNLO**, solid: NLO.

The imaginary part in the CS kernel estimate

- The CS kernel is real-valued.
- The CS kernel *estimate* has a non-zero imaginary part, primarily from matching.
- This is explained by poor perturbative convergence and power corrections in $b_T \Rightarrow$ not treated as a systematic directly
 M.-H. Chu et al. (LPC), PRD 106, 034509, [2204.00200]
 M.-H. Chu et al. (LPC), [2302.09961]
 M.-H. Chu et al. (LPC), [2306.06488]
- Estimates of power corrections expected to improve with multiple lattice spacings, by disentangling $O(a)$ effects
- For this calculation, **uNNLL** dominated by **uNLO** at small b_T – unexpanded matching accounts for power corrections.



$$\begin{aligned}
 & \delta\gamma_q(x, b_T, P_1^z, P_2^z, \mu) \\
 &= -\frac{1}{\ln(P_1^z/P_2^z)} \left(\ln \frac{C_\phi(xP_1^z, b_T, 2xP_1^z)}{C_\phi(xP_2^z, b_T, 2xP_2^z)} \right. \\
 & \quad \left. - (K_\phi(2xP_1^z, \mu) - K_\phi(2xP_2^z, \mu)) + (x \leftrightarrow \bar{x}) \right)
 \end{aligned}$$

Using auxiliary fields for non-perturbative renormalization

Get a renormalized **staple-shaped operator**

$$\mathcal{O}_{\ell,\Gamma}^{\text{ren.}} = Z_{\mathcal{O}_{\ell,\Gamma'}}^{\text{ren.}} \mathcal{O}_{\ell,\Gamma}^{\text{bare}}$$

By solving for Z_0 in a renormalization scheme where it is given by matrix elements computed non-perturbatively, such as

$$\Lambda_{\ell,\Gamma}^{\text{bare}}(p, b) = \langle q(p) | \mathcal{O}_{\ell,\Gamma}^{\text{bare}}(b) | q(p) \rangle_{\text{gf,amp.}}$$

renormalized as

$$\Lambda_{\ell,\Gamma}^{\text{RI}'\text{-MOM}}(p, b) = [Z'_q(p)]^{-1} Z_{\mathcal{O}_{\ell}(b),\Gamma'}^{\text{RI}'\text{-MOM}}(p) \Lambda_{\ell,\Gamma}^{\text{bare}}(p, b)$$

Set to its tree-level value at $p = p_R$, together with some renormalization condition for Z_q . This is **RI'-MOM**, with a different Z_0 for each staple configuration.

¹Green, Jansen, and Steffens, PRL 121 (2018) and PRD 101(2020).

With the auxiliary-field approach, renormalization of extended staples is simplified to that of point-like objects:

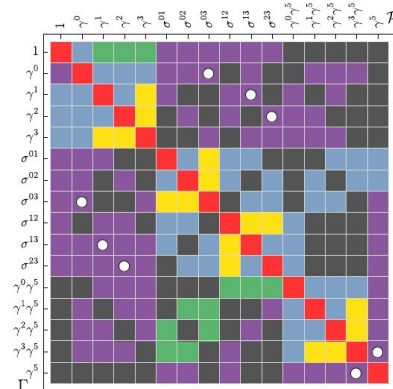
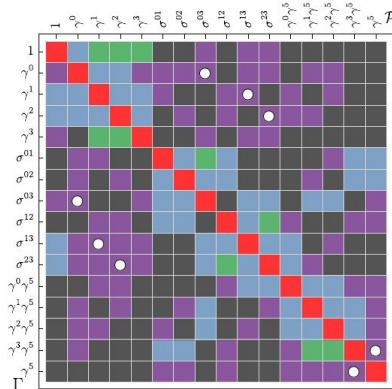
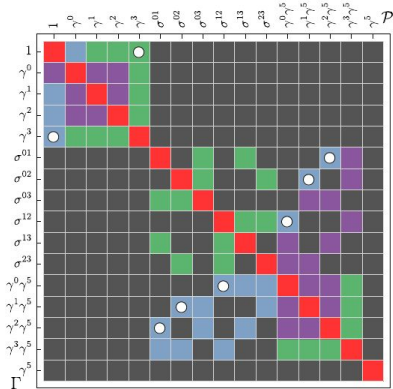
$$\begin{aligned} & \bar{q}(b) \Gamma W_{-z} W_T W_{+z} q(0) \\ &= \langle \bar{q}(b) \underbrace{\Gamma \zeta_{-z}(b) \bar{\zeta}_{-z}(\eta + b_T)}_{W_{-z}} \underbrace{\zeta_T(\eta + b_T) \bar{\zeta}_T(\eta)}_{W_T} \underbrace{\zeta_{+z}(\eta) \bar{\zeta}_{+z}(0)}_{W_{+z}} q(0) \rangle_{\zeta} \\ &= \langle \underbrace{\bar{q}(b) \zeta_{-z}(b)}_{\phi_{-z}(b)} \Gamma \underbrace{\bar{\zeta}_{-z}(\eta + b_T) \zeta_T(\eta + b_T)}_{C_{-z,T}(\eta + b_T)} \underbrace{\bar{\zeta}_T(\eta) \zeta_{+z}(\eta)}_{C_{T,+z}(\eta)} \underbrace{\bar{\zeta}_{+z}(0) q(0)}_{\phi_{+z}(0)} \rangle_{\zeta} \end{aligned}$$

where Wilson lines are given by zeta propagators in the extended theory, and Z_0 is broken down as

$$\begin{aligned} \mathcal{O}_{\ell,\Gamma}^{\text{ren.}} &= e^{-\delta m(l+b_T)} (Z_{\phi_{-z}}^\dagger \Gamma Z_{\phi_{+z}}) \\ &\quad \times \langle \phi_{-z} (Z_{C_{-z,T}} C_{-z,T}) (Z_{C_{T,+z}} C_{T,+z}) \phi_{+z} \rangle_{\zeta} \end{aligned}$$

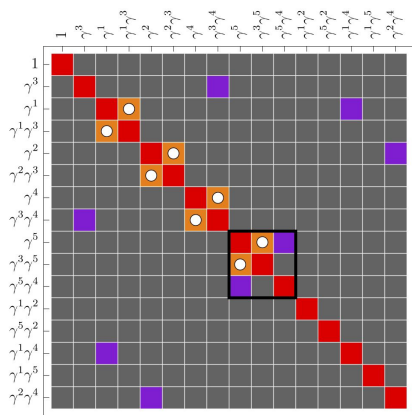
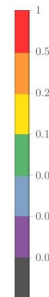
with one renormalization condition for each Z , independent of staple configurations. This is **RI-xMOM**¹.

New renormalization scheme leads to reduced mixing



Figures from Shanahan, Wagman, and Zhao, PRD 101 (2020)

Showing mixing patterns for RI'-MOM from left to right for: straight-line, symmetric, and asymmetric staples.



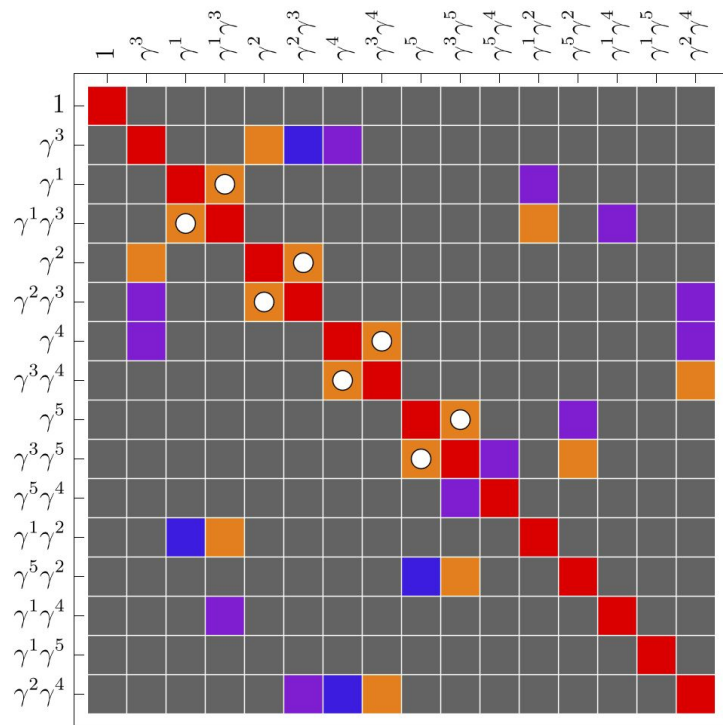
PRELIMINARY

$$p_R^\mu = \frac{2\pi}{L} \times (0, 0, 10, 0), \xi = 0.24 \text{ fm}$$

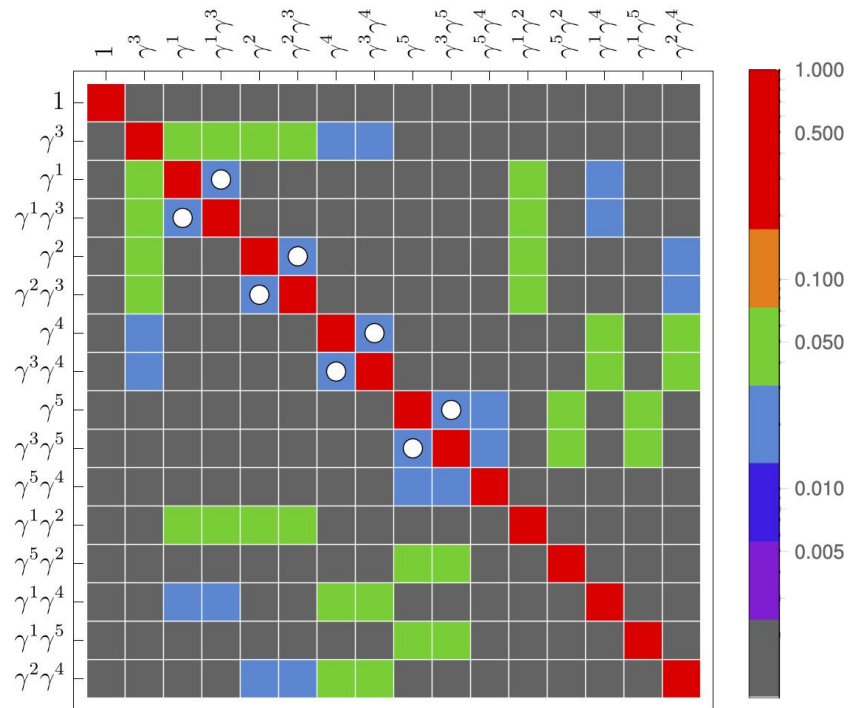
For short, straight-line configurations, mixing patterns in RI'-MOM agree with lattice perturbation theory at one-loop¹ (white circles), but deviations become large for staple-shaped Wilson lines; in comparison, mixing effects in RI-xMOM are well-controlled (for collinear momenta and Wilson lines)

¹Constantinou, Panagopoulos, and Spanoudes, PRD 99 (2019) and PRD 96 (2017).

Scheme dependence of mixing patterns

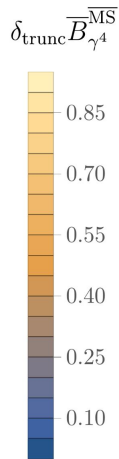
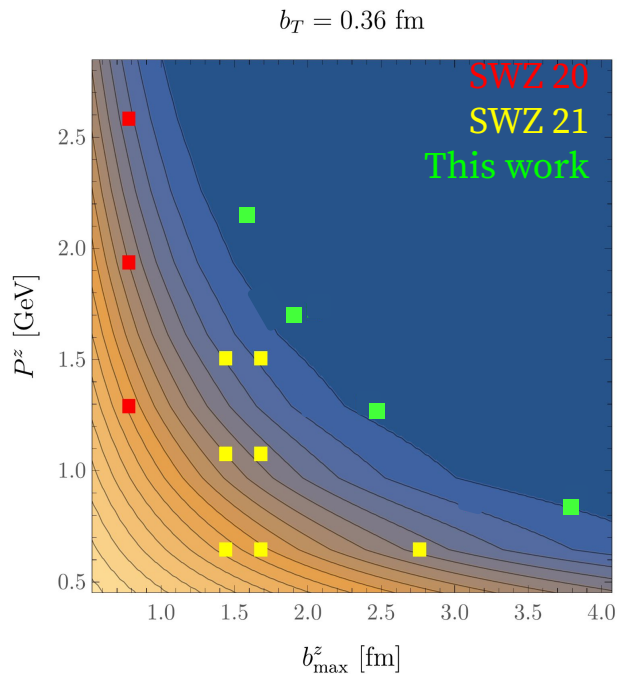


$$p_R^\mu = \frac{2\pi}{L} \times (0, 10, 0, 0), \xi = 0.24 \text{ fm}$$



$$p_R^\mu = \frac{2\pi}{L} \times (6, 6, 6, 6), \xi = 0.24 \text{ fm}$$

Code improvements



Timings for Beam and Wavefunctions

